

Developments of Time Domain Models of Ships, 1997

J M A Spencer

**Report SR 536
August 1998**

Developments of Time Domain Models of Ships, 1997

J M A Spencer

**Report SR 536
August 1998**



Address and Registered Office: HR Wallingford Ltd. Howbery Park, Wallingford, OXON OX10 8BA
Tel: +44 (0) 1491 835381 Fax: +44 (0) 1491 832233

Registered in England No. 2562099. HR Wallingford is a wholly owned subsidiary of HR Wallingford Group Ltd.

Contract

This study was undertaken for HR Wallingford as a part of the company's internally funded research programme. The HR job numbers were DJD0053 and DJD0075. The Project Manager was Dr M W McBride in the Ports and Estuaries Group, which is managed by Dr J V Smallman.

Prepared by


.....
(name)

Senior Math'l Modeller.
.....

Approved by


.....
(Title)

Senior Engineer
.....
(name)

Date 26/1/99
.....
(Title)

© HR Wallingford Limited 2004

Summary

Developments of Time Domain Models of Ships, 1997

J M A Spencer

Report SR 536

August 1998

This report describes various developments that have been made during spring and summer 1997 of HR's computational models for simulating wave forces on and motions of moored ships (UNDERKEEL, DRIFTKEEL, and SHIPMOOR). Developments have been in three distinct areas:

- The extension of UNDERKEEL and DRIFTKEEL to computation of wave forcing, including second-order wave forcing, in short-crested (i.e. multi-directional) seas. Previously, simulations had been restricted to long-crested (i.e. uni-directional) wave conditions.
- Improved representation of steady wind- and current-induced forces on the vessel, and simulation of drag-type damping forces.
- Improved graphical presentation of results using the IDL graphics package.

Verification tests, which demonstrate the models' suitability and accuracy simulating moored ship motions in short-crested wave conditions, have been performed and are reported. It is expected the new improvements will add significantly to the capabilities and hence future usefulness of the DRIFTKEEL and SHIPMOOR models.

Contents

<i>Title page</i>	<i>i</i>
<i>Contract</i>	<i>iii</i>
<i>Summary</i>	<i>v</i>
<i>Contents</i>	<i>vii</i>

1.	Introduction	1
2.	Second-order wave forces in multi-directional waves.....	1
2.1	Force Calculations, Theory	2
2.2	Force Calculations, Implementation in DRIFTKEEL	3
2.3	Force Interpolations.....	3
2.4	Forcing in the Time Domain	4
2.5	Verification.....	5
3.	Drag force computations in shipmoor	5
3.1	Forces caused by Incident Currents and Winds.....	5
3.2	Drag Damping Forces.....	5
3.3	Roll and Yaw Damping	7
3.4	Validation	8
4.	Verification tests in short-crested seas	8
4.1	Physical model test conditions	8
4.1.1	Wave conditions	8
4.1.2	Wind and current forces	9
4.1.3	Water depth	10
4.1.4	The ship	10
4.1.5	Mooring arrangements.....	10
4.2	Computational model test conditions	10
4.2.1	Directional wave characteristics.....	11
4.3	Results	12
4.3.1	Definitions of results values	12
4.3.2	Discussion of results.....	12
4.4	Conclusions	14
5.	Graphical presentation of results	14
5.1	Time History Plots.....	15
5.2	Results Series Plots.....	15
5.3	Extreme Value Plots	16
6.	Conclusions	17
7.	References	18

Tables

Table 1	Verification tests, results comparison: Significant motion values
Table 2	Verification tests, results comparison: Zero-crossing periods of motions.

Contents continued

Figures

Figure 1	Physical model wave basin layout
Figure 2	Motion time history plot
Figure 3	Mooring forces time history plot
Figure 4	Results plot
Figure 5	Extreme value plot

Appendices

Appendix 1	Interpolation of second-order force coefficients in a multi-directional sea
Appendix 2	Sample Unix script for multiple test runs

1. INTRODUCTION

The UNDERKEEL, DRIFTKEEL, and SHIPMOOR models have been developed at HR Wallingford for computing first- and second-order wave forces on stationary ships in shallow water and modelling motions of moored ships. This report describes developments up to October 1997. Earlier development, up to March 1995 is described in Reference 1. Evolutionary development continued after that report was issued, but the individual developments were of a piecemeal nature, and did not in general merit formal reporting.

One significant change made to the DRIFTKEEL model between 1995 and 1997 was the removal elsewhere of the 'Force Rotation Force' calculation. See Reference 1 for a description. The effect has a genuine influence on ship movements and is still reproduced in modelling. However, it is convenient to compute it alongside the other rotational dynamic effects (such as Coriolis and centrifugal forces). Thus it is now found with them in the SHIPMOOR model rather than in DRIFTKEEL. Since in practice, the two models are always used together, the effect of the change is that Force Rotation forces are now computed at a later stage of the modelling process and are not included in DRIFTKEEL output values, but overall modelling results and capabilities are unaffected.

Changes to the models introduced during spring and summer 1997 however have increased the models' capabilities. These improvements have been to three aspects of the models:

- The DRIFTKEEL model has been extended to model the effects of multi-directional waves acting on ships, including second-order wave effects.
- SHIPMOOR has been amended to improve its representation of forces from currents acting on the ship and to incorporate drag forces on the vessel, including drag-induced roll damping.
- Graphics capabilities have been extended and improved using the IDL graphics package.

This report describes the new capabilities and improvements. The provision of multi-directional wave forcing is described in Section 2. The improvements to current-induced force and drag-induced damping forces are described in Section 3. Verification tests, assessing the accuracy of the computational models applied to simulating short-crested wave conditions, are described in Section 4. The new graphics facilities are introduced in Section 5, and conclusions are presented in Section 6.

2. SECOND-ORDER WAVE FORCES IN MULTI-DIRECTIONAL WAVES

A working definition of second-order wave forces is that they are force effects whose magnitude is proportional to the square of wave height. A list of the effects involved, acting on a ship, with descriptions, is given in Reference 1. The forces they generate are not usually large, but they are important because, acting at long periods, they can excite large amplitude horizontal motions of moored ships.

The original version of DRIFTKEEL was restricted to modelling long-crested wave conditions, i.e. wave conditions in which all incident wave energy propagates in one single direction. Diffraction of waves about the ship and radiated waves generated by the ship's movements were simulated, and it has always been possible to simulate randomized wave conditions defined by wave energy spectra. Nevertheless, the restriction to long-crested cases is unrealistic. Waves in nature are not strictly long-crested although refraction tends to align wave crests at coastal sites so that the spread of incident wave directions present becomes small. In such circumstances, the long-crested assumption can be valid as an approximation at least to first-order.

At second-order however, there are grounds for thinking the range of validity of that approximation to be limited. It is known that second-order phenomena, notably set-down wave heights, can be significantly

affected even by modest amounts of directional spreading (Reference 2). Also, it cannot necessarily be assumed that wave directional spreads will be small at all port sites: factors local to some site might limit refractive effects, there might be wave reflections within an enclosed harbour, or surf beat waves reflected off a beach, waves might diffract round both ends of an island breakwater onto a site in its lee, or locally wind-generated waves might propagate on top of a swell from a different direction. Any of these conditions presents a more complicated directional wave pattern than simple short-crestedness can represent.

Therefore, it is necessary to simulate multi-directional seas to simulate moored ship behaviour realistically. In addition, since moored ship behaviour is strongly influenced by long period second-order force effects, which are sensitive to waves' directional characteristics, second-order effects must be incorporated.

It should be noted that introducing multi-directional waves into simulations was in general expected to lead to reductions in forecast ship movements. One of the advantages sometimes cited for the long-crested approach, along with its relative simplicity, is that it is generally conservative. Second-order phenomena tend to decrease in intensity with increasing wave spreads; Reference 2 for example records wave spreads and set-down heights being inversely correlated. However, although being excessively conservative is arguably a less grave error than being wrong in the other direction, it is still a procedural deficiency which leads to over-engineered and unnecessarily expensive design solutions. Experience in using the long-crested model indicated a tendency to over-prediction of ship motions and mooring forces.

Consequently, the DRIFTKEEL model has been modified to simulate multi-directional wave conditions. The remainder of this chapter describes the developments in detail.

2.1 Force Calculations, Theory

The theory involved in expressing second-order wave forces is essentially the same whether the forces are being computed for long-crested or short-crested (i.e. multi-directional) sea conditions. The theory presented in Reference 1 therefore is still applicable. In particular, the expressions derived for the quadratic velocity force, surface stress, and pressure gradient forces are identical:

$$\underline{F}_{VV}^{(2)} = -\frac{1}{2} \rho \int_{S_0} [\underline{u}^{(1)}]^2 dS \quad 1$$

$$\underline{F}_{SS}^{(2)} = \frac{1}{2} \rho g \int_{WL} [\eta^{(1)}]^2 \underline{n} ds \quad 2$$

$$\underline{F}_{PG}^{(2)} = \int_{S_0} \underline{X}^{(1)}(\underline{x}) \cdot \nabla p^{(1)}(\underline{x}) dS \quad 3$$

Where:

S_0	is the wetted surface of the undisturbed hull.
WL	is the equivalent undisturbed hull water-line.
$\underline{u}^{(1)}$	is the first-order water flow velocity.
$\eta^{(1)}$	is the first-order water surface elevation relative to the displaced hull water-line.
$p^{(1)}$	is first-order water pressure.
$\underline{X}^{(1)}$	is first-order displacement (movement) at position \underline{x} on the hull.
\underline{n}	is the unit vector normal to the hull.
ρ	is water density.
G	is gravitational acceleration.

The boundary conditions for the potential flow that generates the 'Motion diffraction' force, and hence the computation and expressions for the force itself, are also unchanged:

$$-\nabla \phi^{(2)} \cdot \underline{n} = (\underline{U}^{(1)} + \nabla \phi^{(1)}) \cdot \underline{\Omega}^{(1)} \times \underline{n} + (\underline{X}^{(1)} \cdot \nabla) \nabla \phi^{(1)} \cdot \underline{n} \quad 4$$

Where:

$\phi^{(1)}$ is first-order flow potential, $\underline{u}^{(1)} = -\nabla\phi^{(1)}$.

$\phi^{(2)}$ is second-order flow potential.

$\underline{U}^{(1)}$ is the (pointwise) first-order hull motion velocity.

$\underline{\Omega}^{(1)}$ is first-order rotation of the hull.

The final effect causing second-order forces is set-down, which in most coastal situations is the dominant effect causing long period drift motions of moored ships. Expressions and procedures involved in evaluating set-down forces, including diffraction effects, are given in Appendix 1 of Reference 1 for the long-crested case, but they are too lengthy to be repeated here. Evaluation methods are identical for the short-crested wave case. Expressions for short-crested incident set-down potentials are slightly different to account for the multiple wave directions; they may be found in Reference 2.

2.2 Force Calculations, Implementation in DRIFTKEEL

In DRIFTKEEL, second-order forces are initially computed in the frequency domain essentially as if calculation were for regular incident waves of unit amplitude. The force coefficients obtained from these calculations are then combined with wave component amplitudes taken in pairs as described in Reference 1, and summed. Invoking standard Fourier Transform theory, the same basic technique can be employed to obtain forces for any required wave condition.

The computation is the same in principle for multi-directional DRIFTKEEL as it is for the long-crested case. Programs for force calculation are unchanged in operation except for the introduction of additional loops over wave direction, requisite amendments to output files, and some fine-tuning to improve computational efficiency, particularly in set-down force calculation, which requires particularly lengthy computations.

In general, the amount of computation and computational time involved in doing multi-directional second-order force computations is a major operational difficulty using DRIFTKEEL. This is due to the enormous number of wave component interactions needing to be represented in a multi-directional sea. The length of computation is such that computation would not have been feasible with computers available at HR before 1997. It is strongly recommended that set-down calculations in particular should be carried out on Ultra Sparc workstations or faster computers (as they become available) if they are at all lengthy. Even then, computational time requirements are still a significant constraint on the number of wave frequency and directional components that it is feasible to represent. As a guide to the time required using 1997 equipment, set-down computations for a fairly moderate set of regular wave conditions in the frequency domain (33 primary wave frequencies, 6 difference frequencies, and 7 wave directions) take about 36 hours to perform on an Ultra Sparc.

2.3 Force Interpolations

After the initial computation of forces in the frequency domain, the next stage in the process of computing forces is interpolation. Because of time constraints, it is possible using DRIFTKEEL to compute force coefficients directly for only a relatively small number of wave frequencies. Interpolating the force coefficients enables the values initially computed for that relatively small number to be applied at the many wave frequencies present in a simulated random sea. Two significant amendments to the long-crested interpolation processes (described in Reference 1) have been made for the multi-directional implementation.

1. The first is a semi-automation of the initial interpolation, in which all force coefficients are interpolated over first-order wave frequencies for fixed values of difference frequencies. This was formerly performed interactively, with human intervention in the process always possible to ensure fitting quality. However, modelling multi-directional seas, the workload required of an operator operating this way would be enormous. For example, consider the fairly modest case of modelling seven wave directions at seven different difference frequencies; this would involve $7^3 \times 6 = 2058$

separate interpolations to be done (7×7 different directional combinations, multiplied by 7 difference frequencies and 6 force components). Paying even only minimal attention to the quality of each individual interpolation, it can be seen an operator would need to spend several hours over the process. Experience using the DRIFTKEEL model shows that in practice the need for manual intervention in this interpolation is infrequent, but if the task extended to several hours, the operator's concentration would very likely flag and intervention when required would not be done well.

Instead, by default, the program now performs interpolations without the operator's intervention and outputs statistics to indicate the quality of fit achieved. The operator then has the option of returning to those suspected of being poor quality to amend and improve interactively as before.

2. The second change is an amendment to the procedure for the second interpolation stage, in which interpolations are made over difference frequencies for fixed primary wave frequencies. The change is technical and complex, and it is therefore not described here. Its description can be found in Appendix 1.

It would in many ways be desirable to interpolate force values over wave direction as well as over frequencies. Doing this would in principle enable continuous directional distributions of wave energy to be simulated and thus allow further enhanced realism in ship modelling. Some such interpolation is foreseen as a future development of the model. At this stage however, it is considered that the difficulty of verifying the quality of the interpolation would be too great, that the computational effort required to compute the final forcing time series in a continuous wave energy directional distribution would be too much, and that, in general, the extra complication of the program it would involve would be too great for it to be feasible. The present version of the DRIFTKEEL model does not attempt a continuous directional distribution of wave energy. Instead, the directional energy distribution is given a discrete interpretation with waves propagating in only a finite number of specified directions (at present this is restricted to 12 by array dimensions in the program).

2.4 Forcing in the Time Domain

The final stage of the process in DRIFTKEEL is to take the force coefficients computed earlier in the frequency domain, interpolated to cover any relevant wave and difference frequencies, and from these coefficients to compute wave forcing sequences. The method of producing these sequences to simulate the action of random waves on a ship at its berth realistically is described in Reference 1 but is reiterated in brief below:

1. Incident waves are represented in the frequency domain as a Fourier series of complex components. Component values are set by probabilistic rules: each is assumed to be normally distributed with variance proportional to the incident wave spectrum. The probabilistic distribution ensures wave simulations and force sequences have the correct stochastic properties to reproduce natural variability.
2. These wave coefficients are then multiplied by the force coefficients calculated by UNDERKEEL and DRIFTKEEL. First-order forces require only simple multiplication. Second-order force coefficients are multiplied by wave coefficients taken in pairs at the appropriate difference frequency and summed. The required outcome is a Fourier series of forces corresponding to the random waves.
3. Finally, the force Fourier series is inverse transformed to give a random forcing sequence in the time domain.

The process is repeated for each of the six components of force on the ship, employing the same wave coefficients to represent the same incident wave sequence in every case.

The method is the same in principle in multi-directional sea simulations as it is in long-crested. In the short-crested case though, there are more wave and force coefficients, and summations to take account of waves and forces generated by waves propagating in different directions.

2.5 Verification

Tests undertaken to verify the DRIFTKEEL model applied to short-crested, multi-directional wave conditions are described in Chapter 4.

3. DRAG FORCE COMPUTATIONS IN SHIPMOOR

3.1 Forces caused by Incident Currents and Winds

As originally written, SHIPMOOR did not have any explicit facility to model wind and current forces acting on a moored ship. Instead, it was necessary for an operator to hand-calculate forces, and then input values as constant forces that acted on the vessel. Typically, the calculation was made using equations and drag force coefficients taken from Reference 3.

Hand calculation of forces for SHIPMOOR was a tedious chore, and sometimes a source of error in modelling, especially when a test series required modelling many different wind and current conditions. It was therefore decided to automate the process and incorporate computation into the computer program.

Computation is a straight application of the method given in Reference 3. Drag force coefficients that vary with wind and current direction and under-keel clearance (in the case of current forces) are used, incorporated into SHIPMOOR stored in look-up tables. These, the program interrogates as required and interpolates for the required direction and under-keel clearance of the wind or current and vessel being modelled. Wind and current speeds are taken relative to the ship. Forces and moments are then computed from vessel dimensions, those speeds and the coefficients by applying the drag force equations (given in Reference 3).

A shortcoming of the implementation is that the coefficients used were derived for use in estimating forces on moored VLCCs, and it could be argued they are not properly applicable to other classes of ships. However, suitable reliable alternative data is unfortunately scarce. As and when force data for other ship types becomes available, it can be incorporated into the model and used as an alternative.

In principle, the method could be used to simulate turbulent currents and wind gusts by allowing current and wind velocities to vary in time. It is not however used in that way in the present version of the program. The present version of the program permits only steady incident winds and currents although the forces' dependence on *relative* current velocities does give some time-variation and effectively a damping force.

3.2 Drag Damping Forces

As a side effect of the implementation of the current force calculation described above (and also, but to a much lesser extent, the wind force), SHIPMOOR also now includes some drag-type damping force on the ship modelled.

Current and wind force equations taken from Reference 3 are all of the general 'drag' form:

$$F = \rho A C_D V |V| \quad 4$$

Where:

A is a cross-sectional area.

V is current speed relative to the hull.

C_D is a drag coefficient.

V is current speed relative to the hull; that is, if U_S is the hull's speed of motion and U_C is current speed over the ground:

$$V = U_C - U_S \quad 5$$

Substituting into the drag force equation and re-arranging signs, the general form for drag damping on a moving body in a current is obtained:

$$F = - \rho A C_D (U_S - U_C) |U_S - U_C| \quad 6$$

The simplest, most familiar form of the drag damping equation can be obtained by considering the zero current case, $U_C=0$. Then:

$$F = - \rho A C_D U_S |U_S| \quad 7$$

... or it can be obtained in a more general fashion by defining V_S to be the ship's speed through the water: $V_S=U_S-U_C$, and then:

$$F = - \rho A C_D V_S |V_S| \quad 8$$

The expression above (Equation 9) represents precisely the same force as the current force expression first given (Equation 5), which is employed in the SHIPMOOR model. One is written in 'drag damping' form and the other as 'current force', but they are exactly equivalent. This observation shows that the formulation of current forces employed in SHIPMOOR, which uses current velocities relative to the ship, at the same time also automatically represents drag damping forces on the ship.

However, the drag coefficients the program uses were derived for Reference 3 for use in steady state situations; they might not be accurately applicable to calculating time-varying drag forces. Drag forces commonly require some time to evolve as the physical processes that cause them (principally flow separation for classical drag on an immersed body) develop. As flows around a body change, therefore, drag forces in the body, and drag coefficients, can appear to lag behind. In addition, drag coefficients that apply to steady-state flow situations, in which flow is fully developed, are not necessarily applicable to unsteady flows and motions.

Given this factor, it might be more accurate to adopt 'unsteady flow' force coefficients for use in the model. Defining what might be suitable values however is not straightforward. The general relationship between drag and velocity is extremely complicated. In regular reciprocating flows or body motions, coefficients can be regarded as being functions of frequency and Keulegan-Carpenter number (the dimensionless ratio of body dimension to flow orbit length). But in random motion no such relatively clear-cut relationship exists. Therefore, in a random sea, such as SHIPMOOR simulates, there is no one obviously applicable drag coefficient value to use. Given these circumstances, for simplicity and for modelling steady current forces correctly, choosing the steady-state value seems reasonable.

It should also be noted that some proportion of the 'drag' current force exerted on a moored ship is due to free-surface wave effects rather than to 'classical' drag, i.e. the drag force associated with separated water flows within the body of the water. Waves generally form on a water surface as it flows past an object, for example, a moving ship or a bridge pier in a flowing river. These waves transport energy away from their site of generation, and they therefore must exert a damping force on any moving object. This is an additional wave effect, distinct from any of the first- and second-order effects modelled in DRIFTKEEL. A simple dimensional analysis shows the force to be proportional to speed squared, like drag. Since they have this factor in common, it is assumed this free-surface force is subsumed within the drag force for the purposes of calculation in and from Reference 3.

The two forces, however, do not vary by the same rules. The free-surface force is Froude number dependent whereas drag force is related to Reynolds number. For this reason, there are difficulties adequately

representing both in scale physical models. It is expected that accurate compensation was made in interpreting the physical model test results from which the coefficients presented in Reference 3 derive.

The size of the free-surface force component has not been separately estimated for a moored ship. It is however analogous to the 'wave making resistance' to ships in forward motion. As that is known to be a major contributor to the total resistance force on a moving ship, it can be assumed the free-surface effect is significant, at least to surge forces in fore-aft ship motions.

Like classical drag, the free-surface force will take time to evolve as waves develop around a moving ship, so steady-state coefficients are not necessarily applicable to non-constant conditions. The force can be expected to be dependent on frequency and Keulegan-Carpenter number in regular reciprocating motion. Similar arguments apply to the applicability of frequency- and Keulegan-Carpenter dependent coefficients to this wave-making force in random motions as were outlined above for drag forces. Again, use of steady-flow coefficients, although not ideal, is considered reasonable.

For the various reasons outlined above, the precision of the drag force representation now employed in SHIPMOOR is uncertain. Given the various inherent uncertainties involved in simulating drag in randomly varying flows and motion however, it seems at least a reasonable interim approximation. Validation against experimental data is awaited.

3.3 Roll and Yaw Damping

The current force calculation does not automatically give damping forces in heave, pitch, roll and yaw in the same way as it does for surge and sway because there are no currents flowing past the ship that correspond to the motions in the same way. In the cases of heave and pitch, this is unimportant, because drag forces affecting these motions are relatively insignificant compared to inertial and buoyancy effects. However, drag-type damping is known to influence roll motion significantly. Therefore, an attempt has been made to incorporate the effect into the SHIPMOOR model. A similar method is also used to estimate yaw damping forces.

It is assumed that pressure is distributed over the sides of the vessel strictly proportionally to velocity-squared, and that under-keel pressure distributions do not contribute to roll drag. Rotation is taken to be about the centre of mass of the vessel. After these assumptions, if the ship has draught d and the centre of mass is at a height z_g above the keel, roll velocity is ω_1 , the roll drag damping moment is given by:

$$M_I = -\rho L C_D \int_{z=0}^d |z - z_g|^3 \omega_1 |\omega_1| dz \quad 9$$

If the centre of mass is beneath the water line, this equals:

$$M_I = -\rho L C_D \frac{z_g^4 + (d - z_g)^4}{4} \omega_1 |\omega_1| \quad 10$$

Otherwise, if the centre of mass is above the water line, it is:

$$M_I = -\rho L C_D \frac{z_g^4 - (d - z_g)^4}{4} \omega_1 |\omega_1| \quad 11$$

Similar considerations give a yaw drag moment if the centre of mass is assumed to lie at midships of a vessel length L :

$$M_6 = -\rho d C_D \frac{L^4}{32} \omega_3 |\omega_3| \quad 12$$

It is assumed the same drag coefficient, C_D , is applicable to roll and yaw damping as to sway. The assumption is certainly questionable, for reasons including those given in the preceding section of this report. However, as a working hypothesis, it is tenable until better data can be incorporated, which it is hoped to do in the near future.

3.4 Validation

The functions for drag forces in surge and sway, and rolling and yawing moments described in this chapter were incorporated in the version of the SHIPMOOR program that was used during the tests described in Chapter 4, below. Those verification tests therefore served to validate those modifications in addition to their primary purpose of verifying the multi-directional wave forcing computations. It can also be noted that the drag force and yaw moment expressions used here were taken from a published source (Reference 3) and are well established in use predicting loads on ships in steady currents. Their validity in that application was therefore established prior to their installation in SHIPMOOR.

4. VERIFICATION TESTS IN SHORT-CRESTED SEAS

The tests performed to verify the accuracy of the multi-directional version of UNDERKEEL reproduced physical model tests originally undertaken in connection with a commercial project. Having been originally conducted for a different purpose, these tests were not ideal for the purposes of verification. A level seabed and simplified mooring arrangement like that employed in verification tests for the earlier version of DRIFTKEEL (Reference 1) would have been preferable. However, the physical model tests were well documented with a complete set of results readily available, and they were considered adequate for the purpose.

4.1 Physical model test conditions

The layout of the wave basin in the physical model tests is shown in Figure 1. The model was constructed to a scale of 1:100 (in both vertical and horizontal directions) and the seabed area represented was approximately 1700m by 1700m. The bed topography consisted of a simulated gently sloping seabed with a deeper dredged entrance channel and turning and mooring areas. The wave paddle was placed in any of three alternative positions to simulate waves from different offshore directions. The paddle was a multi-element one, thus allowing short-crested waves to be generated in the basin.

4.1.1 Wave conditions

A summary of inshore wave conditions forecast for the site and simulated in modelling is given below:

Inshore Direction	215°			192°			169°		
	H _s (m)	T _p (s)	U ₁₀ (m/s)	H _s (m)	T _p (s)	U ₁₀ (m/s)	H _s (m)	T _p (s)	U ₁₀ (m/s)
52/1 yr	-	-	-	2.1	7.2	10.2	1.7	6.4	9.2
24/1 yr	0.9	5.1	7.2	3.1	8.8	12.5	2.5	7.9	11.6
18/1 yr	1.3	5.9	8.6	3.4	9.2	13.1	2.8	8.4	12.3
10/1 yr	1.9	6.8	10.6	4.1	10.1	14.3	3.4	9.2	13.5
6/1 yr	2.4	7.7	12.0	4.6	10.7	15.2	3.9	9.9	14.4
1/1 yr	4.0	10.1	15.3	6.3	12.8	17.5	5.6	12.2	17.0
1/50 yrs	7.3	13.5	20.0	9.5	15.7	21.2	8.9	14.9	21.1
1/100 yrs	7.8	14.0	20.7	10.0	15.8	21.7	8.9	14.9	21.7

Random waves in the physical model were generated by means of a synthesizer. Conditions were specified in terms of Pierson-Mosowitz wave spectra, scaled down when necessary to give the correct, required wave height. Conformity of wave conditions with the specified spectra was checked by measurement during tests using wave probes situated close to the wave paddle.

Mean wave directions are given above defined relative to the axis of the moored ship. Generated wave conditions were short-crested; each thus contained components propagating in a range of different

directions. The direction given here is the mean direction of propagation, i.e. the mean direction the wave energy is going *to* rather than the meteorological convention of the direction the wave is coming *from*.

The short-crested directional characteristics of waves are conventionally expressed in terms of a directional wave spectrum, $S_{\theta}(f, \theta)$, which represents the energy density of waves at frequency f propagating in direction θ . In this case, a nominal exponential spreading function, $g(\theta)$, was adopted, so that the directional spectrum, $S_{\theta}(f, \theta)$, of the waves could be expressed as the product of $g(\theta)$ and the ‘non-directional’ spectrum, $S(f)$:

$$S_{\theta}(f, \theta) = g(\theta) S(f) \tag{14}$$

Where, incorporating a directional spread parameter, σ , and a mean direction, θ_0 :

$$g(\theta) = \frac{1}{\sqrt{\pi\sigma}} e^{-\frac{(\theta-\theta_0)^2}{\sigma^2}} \tag{15}$$

However, it is not possible in practice ever to produce a continuous directional energy distribution like the one above using a wave paddle that has only a finite number of paddle elements. So although the continuous exponential above was the nominal ideal, the actual distributions produced in tests were discrete approximations in which waves propagated in only a finite number of directions. Both physical and computational model tests employed discrete distributions, but different approximations were employed in the two cases (see Section 4.2.1).

Directional spread values simulated, which differed between tests involving waves from different incident directions, were:

Mean wave direction, θ_0	Spread, σ
215°	24°
192°	27°
169°	24°

4.1.2 Wind and current forces

Wind and current loads on the ship were estimated by the method and formulae given in Reference 3 and were represented in physical model tests using weights attached to the vessel by thin twine acting over pulleys.

The wind speeds represented are given in the U_{10} column of the wave condition table (above). Directions offshore were coincident with mean wave directions, but refraction altered wave directions during their inshore propagation, so wind directions were different from inshore wave directions. Wind directions at the berth site, relative to the ship, were as follows:

Mean wave direction, θ_0	Wind direction
215°	225°
192°	195°
169°	165°

The simulated current in all tests was 0.7kts acting off the berth.

4.1.3 Water depth

A still water level of +2.86m CD was represented in all tests, which when combined with a nominal dredged bed level of -14.0m CD gave a water depth of 16.86m at the berth.

4.1.4 The ship

The model ship represented, at 1:100 scale, a modern LNG tanker, principal dimensions of which are given below. In the verification tests, it was simulated in its design, fully loaded state:

Length, between perpendiculars	277.0m
Length, overall	293.0m
Breadth	46.0m
Moulded depth	26.0m
Design draught	11.0m
Design displacement	103,385t

4.1.5 Mooring arrangements

The mooring plan used in the physical model tests is shown in Figure 1. The height of the tops of the mooring dolphins was +10.0m CD.

Each line shown on the mooring plan represents a group of two or three in prototype. In physical model tests performed at the start of the test programme, all groups consisted of two lines, but the number in some groups was later increased. Thus, of the tests reproduced for computational verification:

- In Tests 7, 8, 9, and 11, all groups consisted of two lines
- In all other tests (i.e. Tests 12, 13, 14, 15, 23, 24, 25, 26, 27, 28), Groups M1 & M5 had three lines, while all other groups consisted of two.

All mooring lines were, in prototype, steel wires with nylon tails. The breaking load of each steel wire was taken to be 126t, at which it was assumed to be stretched by 1.5% of its original, unstretched length. The active length of the tails was taken to be 10m, which, since part of the tail would be looped around the mooring bollard, was equivalent to an overall length of about 11m. For the nylon tails, 85mm diameter rope was assumed with a mean breaking load (MBL) of 160t and 17% extension at 80% of MBL. In the physical model tests, mooring lines were represented by fine wires attached to springs with the requisite elasticity for each mooring line group.

Two fenders were also represented, as shown on the mooring plan. Since exact fender characteristics were anticipated not to be critical to moorings' performance, these were simulated approximately, by linear springs with stiffness equivalent to 1200t/m.

4.2 Computational model test conditions

The aims of the computational model tests were:

1. To replicate the physical model tests described in section 4.1 as closely as possible, and thus ...

2. To assess the accuracy of the computational models by comparing results.

Only the part of the original test programme comprising tests involving the fully laden ship moored by steel wires with tails and mooring dolphins in just one of the two alternative locations was selected for reproduction in this way. Other tests, which involved either the ship in ballast, all wire mooring lines, or dolphins in the other positions, were not re-simulated.

Each of the chosen tests was re-run as a computational simulation using the DRIFTKEEL and SHIPMOOR models as described elsewhere (see e.g. Reference 1) and with the same simulated ship, mooring and environmental conditions as described in Section 4.1.

Fenders were modelled in the computational model as being friction-free. The precise friction characteristics of the fenders used in the original physical model tests are unknown, so it is unclear how best to simulate them. However, it is usual to minimize friction in fenders in physical modelling, so the assumption is probably not unrealistic.

Computational test lengths were 4608 seconds in total, with a 0.25 seconds time-step. However, the first 512 seconds were not used for analysis, to allow for transient effects at the start, so the effective length of every test run was 4096 seconds (1.14 hours).

4.2.1 Directional wave characteristics

In doing the verification tests, particular emphasis was placed on reproducing wave conditions with short-crested directional characteristics that were as like as possible to those in the original physical model. However, the representations of the directional distribution of wave energy differ significantly between the physical and the computational models. In both, the continuous distribution that exists in reality (expressed by the $g(\theta)$ function in equations above) is approximated by a discrete distribution of wave energy. But the discretisations are different.

The physical model is set up so that the wave basin acts as a wave-guide along which waves can propagate at only certain discrete angles to its principal axis. These directions depend on the width of the basin, and also on water depth and wave period. Different frequency components of the wave spectrum therefore propagate at different angles.

In the computational model, on the other hand, the wave directions are a finite set of up to thirteen prescribed by whomever is running the model, and the same set of wave directions is represented at all frequencies. In the case of these verification tests, the directions ranged between 132° and 252° (relative to the axis of the moored ship) at 10° intervals. The central direction was thus 192° , the same as the central one of the three mean wave directions tested (215° , 192° , and 169°).

Initial test results showed relatively large discrepancies between physical and computational model ship motions in tests of waves at the 169° mean direction. In an attempt to rectify this discrepancy, an additional short series of computational model tests (Tests 12', 13', 14', 15') was performed with computational wave directions centred on 169° , i.e. directions ranging from 109° to 229° at 10° intervals. Results, however, were not significantly different from the first series'.

In general, several different directions are possible for wave propagation at any frequency in either model, and the proportions of wave energy allocated to each direction are weighted to approximate as closely as possible to the directional distribution specified. Both the physical and the computational models can thus be made to approximate (discretely) to the same (continuous) nominal directional distribution. However, the approximations differ in detail because representable wave directions depend on frequency in the physical model and not in the computational model, so the sets of wave directions present in the two models are, in general, different.

Thus it is not possible for the computational model identically to replicate conditions in the physical model. Instead, it generates similar wave conditions that simulate the same prototype conditions with the same frequency spectrum and equivalent directional characteristics.

4.3 Results

Test results are summarized in Table 1, showing ‘significant motion’ values, and Table 2, which lists zero-crossing periods. Values are in metres for surge, sway and yaw significant motions, degrees for roll, pitch and yaw, and seconds for all zero-crossing periods. The significant values published for heave motions in physical model Tests 8 and 9 appear to have been misprinted in the original report and have been disregarded.

Results are not presented for mooring forces because the only values published for the original physical model tests were maximum values recorded during tests. In randomized wave tests, maximum values can be naturally very variable. They therefore do not constitute a reliable basis for comparison between the models.

Test Numbers refer to the order in which the original physical model tests were performed and are not significant here except as indices. Tests are presented here in order of increasing incident wave height with tests of waves from the same mean direction grouped together. Note that wave conditions were identical for Tests 8 and 28, and Tests 9 and 27; however, the mooring arrangements were different (see Section 4.1.5).

4.3.1 Definitions of results values

‘Significant motions’ are defined here, analogously to significant wave heights, as four times root mean square values, thus:

$$x_s = 4 \sqrt{\frac{1}{N} \sum_{i=1}^N (x_i - \bar{x})^2} \quad 16$$

Where: $x_i, i=1,2,3, \dots, N$ represents the time sequence of N position values computed in the test run.

\bar{x} is the mean of the x_i values .

In both tables of results, values taken from the physical model test results are listed for comparison with computational results. Tables also present a relative error percentage, which is defined thus:

$$Err = \left(\frac{X_C - X_P}{X_P} \right) \times 100\% \quad 17$$

Where: X_C is the value (significant motion or zero-crossing period) obtained from the computational model

X_P is the equivalent value obtained from the physical model

Defined in this way, positive values of relative error indicate computational model values greater than the physical model’s, so the computational model is yielding an over-estimate, while negative values indicate under-estimation.

4.3.2 Discussion of results

Inspecting the tables of results, the quality of agreement achieved between computational and physical model test results is generally good, except for pitch significant motions, for waves in the 192° wave

direction. It is less good for tests of waves in the 215° direction, and it is poor for waves at 169°. The discrepancies in the 169° results are not significantly smaller in the repeat test series (Tests 12', 13', 14', 15') with computed wave directions centred on 169° than they were in the original test series with directions centred on 192°.

The reason for the pitch response discrepancy is unknown. However, the relatively short zero-crossing periods given in Table 1 indicate that the response is primarily first-order, as is typical of pitching motions of ships. Thus, it is very likely that any error will be associated with first- rather than second-order effects. Pitch responses can be sensitive to small variations in damping and added inertia at and around resonant frequencies, and this is one possibility to account for the discrepancy. Another possibility would be differing excitations due to the different incident wave directions present in the physical and computational models discussed in Section 4.2.1.

A slightly better quality agreement of results for waves at 192° than for either of the other two directions tested was expected. This was because, at least initially, the incident wave directions selected for computation of forces in DRIFTKEEL (set out in Section 4.2.1) centred on the 192° direction, and the force computation was thus optimized for simulating wave forcing for that direction. However, it is not known why agreement should be better for waves at 215° than for waves at 169°.

The range of directions for which forces were computed in DRIFTKEEL was wide enough to encompass nearly all the activity of incident waves in the 215° and 169° directions, even taking into account the directional spread of 24°. Further, in the tests of waves at 169°, centring computed wave directions on 169° (Tests 12', 13', 14', 15') rather than 192° did not lead to a significant change in ship movement magnitudes. If there were inadequate coverage of the spread of wave directions in the computations, the 169°-centred simulations would include significantly more of the wave activity in these tests and therefore generate more ship motion than would the 192°-centred ones. Thus, the idea that significant wave forcing from wave activity at the extremes of the directional range might have been omitted in the tests of waves at 215° and 169° mean directions and that this led to under-estimation of forcing does not appear to be true.

Looking at the wave basin layout (Figure 1), the most significant feature distinguishing the 169° from the other wave conditions is that waves must propagate across the navigation channel before reaching the ship at the berth in the 169° tests. This is a feature that might account for the greater discrepancies between physical and computational model results at 169°. It is probable that wave reflection and refraction effects take place as waves cross the deeper water channel. The effects could influence and change wave conditions and hence the forces on the moored ship. Hence the vessel's motions would be affected. Furthermore, if the wave effects are produced in the wave basin but not reproduced in the computational model, this factor could account for the observed discrepancies between physical and computational model test results at 169°. And in addition, the discrepancies can be expected to be less in waves at other directions, when refraction and reflection are presumed to be less significant.

Broadly, two kinds of wave effect are possible crossing the channel:

1. Refraction and reflection may transform incident waves as they travel across the steep side slopes of the entrance channel or turning basin. They might for instance: alter waves' directions of travel, induce wave breaking, change wave heights by shoaling, produce standing waves, or cause wave scattering. Any or all these would alter incident wave forcing on the moored vessel and consequently ultimately affect its movement.
2. The transformed waves, particularly long wave components, instead of propagating away and being dissipated as in nature, can become trapped in a wave basin. The trapping is done by reflections off the surroundings: the wave paddle, wave guides and spending beaches (which do not always dissipate long wavelength waves effectively) do not allow waves to escape. Once trapped, the waves are spurious. A pure experimental artefact, they do not equate to any waves found in nature, and neither are they

present in the computational model. However, if they are present in the physical model, they affect ship motions and induce erroneous results and discrepancies.

A third potential possibility is that other hydrodynamic effects due to the unevenness of the seabed about the ship could affect ship motions. Being based on a fundamental assumption that the bed is level, the computational model cannot replicate these. However, the possibility can probably be discounted since any such effect would also be likely to influence responses in all other wave conditions, not just those at 169°, and there is no evidence of that occurring.

It should be noted that neither of the first two possibilities would indicate a shortcoming in the computational model if it were true. The second, the possibility of spurious wave activity, would be a fault in the physical modelling. The first, that waves are changed as they approach the berth across the channel, can be viewed as being essentially a problem in forecasting the incident wave conditions: presumably, were DRIFTKEEL supplied with correctly transformed waves, the consequent ship movements would be simulated correctly. Unfortunately, it is not possible to adjudge from the data that is available which, or whether either, of the possibilities pertains, and the discrepancies between physical and computational model test results therefore remain at present incompletely resolved.

4.4 Conclusions

The possibilities discussed in the two paragraphs above illustrate the desirability of conducting verification tests in the simplest and most controllable conditions possible. In this case, the complication was that the seabed was not level. Because of the non-level bed, different possibilities to account for observed discrepancies in results cannot be ruled out, including either experimental error in the physical model or uncertainty in the force input data appropriate for the computational model.

In the tests of waves at 192° however computational and physical model results were in good agreement. This was the wave direction in which the influence of seabed topography affecting the ship response was minimal, and for which both the physical and computational models were optimized. In addition, there are likely reasons to account for the largest observed discrepancies between physical and computational model results, those in 169° wave conditions, that do not imply any shortcoming in the computational model. The results of this verification exercise therefore, whilst not absolutely conclusive, are encouraging. They strongly suggest that the developed multi-directional version of DRIFTKEEL can be used in appropriate circumstances accurately to forecast motions of moored ships in short-crested wave conditions including long period second-order force effects.

5. GRAPHICAL PRESENTATION OF RESULTS

Fairly recently, IDL has become the standard computer graphics package for use at HR. This has prompted a review and revision of results output, particularly graphical output, from the SHIPMOOR model, which was written several years ago using Ghost graphics routines. At the same time, the work presented in Reference 4 has suggested new approaches to undertaking testing and analysing results, doing multiply repeated test runs to obtain statistically more valid results by a method of computational experiment. This new approach also requires a different approach to results' presentation if it is to be used with maximum efficacy.

IDL operates on distinctly different principles from Ghost. It is designed for post-processing of data, whereas Ghost is a set of subroutines that are incorporated into and processed as an integral part of a Fortran program (in this case, SHIPMOOR). Used with IDL, results computed by SHIPMOOR are written temporarily to file for subsequent reading and processing by an IDL program (or procedure).

At present, IDL and associated Fortran programs are available for presenting three distinct classes of results:

1. Graphs plotting the history of ship movement and mooring forces through an individual test, similar to the plots that were available previously using Ghost.

2. Plots showing variation of ship movement or mooring forces (e.g. rms or maximum values) plotted against an environmental parameter (e.g. significant wave height, direction or wind speed). Results obviously need to be taken from test series in which the parameter is varied systematically.
2. Extreme value plots of ship movement and mooring force used to determine probabilistic aspects of ship response as described in Reference 4.

5.1 Time History Plots

In the Ghost version of SHIPMOOR, a plot of the time history of vessel movement was always generated as part of every SHIPMOOR test run's output, and a plot of mooring forces' time history could be obtained as an option. In the IDL version, both are available as options.

Time history plots can be useful in de-bugging the SHIPMOOR model: for example, errors in setting-up mooring data or the impulse response function can show up in characteristic ways in time histories. They are also commonly required for purely illustrative purposes in reports. However, the output files involved can be large, leading to problems finding sufficient file storage space, and it is usually preferable not to generate them unless certain they will be required. As now implemented, the user may choose in SHIPMOOR to plot either ship movement or mooring force time histories or neither or both from any test run.

Vessel movement time history plots are obtained by entering any of 'i', 'I', 'w', or 'W' in the option list line of the SHIPMOOR control data input. SHIPMOOR will then automatically create and open a file (output on channel 10) with a name specified by the user (SHIPMOOR control data input 'IDL file') and the extension '.mot'. The ship's position and orientation is recorded in this file at every time step. Once the run is completed, time history graphs can be plotted using the IDL procedure 'seqpro'. An example of the resultant output is shown in Figure 2.

Mooring force time history plots are obtained similarly. The option 'm' or 'M' is required in the SHIPMOOR option list. Mooring line and fender forces are written at every time step to a file which is automatically created and opened for output (on channel 11) with the same user-specified name specified by the 'IDL file' control data input but extension '.mor'. The IDL procedure for plotting mooring force time histories is 'morseqpro'. An example of output is shown in Figure 3.

5.2 Results Series Plots

When, as is good practice, SHIPMOOR tests are conducted in ordered series with environmental parameters systematically varied, utility programs are available to extract results values from the standard SHIPMOOR output files and present them graphically. An example of output is shown in Figure 4.

The first utility program to use is 'xtplot', which is a Fortran program that extracts the specific and specified required results from standard SHIPMOOR results files and stores them in a format suitable for IDL plotting. Using xtplot, the user can select any of the following results values, obtained by spectral analysis, to plot:

- Root mean square (rms)
- Significant value ($4 \times \text{rms}$)
- Rms from zero (i.e. variation from zero rather than mean value)
- Significant value from zero
- Mean zero-crossing period (T_m)
- Spectral peak period
- Mean value
- Maximum value observed
- Minimum value observed
- Extreme value (i.e. the larger of the absolute values of maximum and minimum)
- Range value (i.e. the difference of the maximum and minimum)

For some of these, it is also possible to choose to plot values derived from only either high or low frequency range responses.

The user also selects one of the following possible parameters as the independent variable against which the results are plotted:

- Significant wave height
- Wave direction
- Current speed
- Current direction
- Wind speed
- Wind direction
- Passing ship speed

And the user inputs a list of names of SHIPMOOR standard output files containing the results of the test series. From these, xtpplot extracts the relevant values and prepares them for plotting.

Plotting uses the IDL procedure, 'valpro'. Figure 4 shows an example of output obtained using the valpro procedure. Valpro plots the selected results' values against the environmental parameter. An alternative presentation, applicable only to mooring force value results, is available using the procedure, 'linfo' (not illustrated).

5.3 Extreme Value Plots

A powerful test method applicable to test conditions in which maximum or extreme response values need to be forecast is described in Reference 4. The forecasting of extreme responses is particularly prone to uncertainty because of the stochastic nature of moored ships' motions in waves and because the extreme values in tests are statistics that are particularly subject to variability. It is not usually possible to establish absolute extreme values that are never surpassed. Forecasting extreme values therefore demands a probabilistic approach. However, under the combined influence of mooring lines, fenders and second-order wave effects, the probability distributions describing extreme values of moored ship response are incompletely known and understood, so forecasting from purely theoretical principles is not feasible. In practice, it is conceptually and practically simplest to adopt an experimental approach to forecasting.

The method involves executing a large number (possibly several hundred) of repeat tests with environmental conditions that vary stochastically. That is, although conditions differ between runs, conditions are statistically similar. For example, a test series might be performed, as described in Reference 4, each with a different simulated wave sequence but the same (expected) wave spectrum.

Maximum and minimum values of ship responses and mooring forces from each test are recorded and can be plotted against cumulative probabilities using the so-called 'extreme probability rule' (see, e.g., Reference 4). It should be found that the plotted data fall in an approximately straight line, the calculated slope and y-intercept of which imply the probability distribution of the plotted test values and hence of the extreme values of the ship motion. Once this distribution is known, the extreme vessel motions can be forecast, as is described in Reference 4.

A sample Unix script used to perform multiple tests and extract required results is given in Appendix 2. Values can then be analysed and plotted to estimate probability distributions, expectation and maximum likelihood values of extrema using the 'xvalan' Fortran program and the 'xvpro' IDL script. An example of the type of plot that is obtained is shown in Figure 5.

6. CONCLUSIONS

A number of significant developments have been made during spring and summer 1997 to the UNDERKEEL, DRIFTKEEL and SHIPMOOR models used to simulate wave forces on moored ships and their movements in response. The developments comprise:

1. A facility to simulate wave forcing, including second-order wave forcing, due to short-crested waves, i.e. sea conditions with waves propagating in more than one direction (UNDERKEEL and DRIFTKEEL).
2. Improved representations of wind and current forces on a moored ship, which as a side-effect also represent drag damping forces on the vessel acting in surge and sway (SHIPMOOR).
3. Representation of roll and yaw drag damping moments on the ship in motion (SHIPMOOR).
4. Improvements to graphical output from the model incorporating the use of IDL, which is now the HR standard graphics, package (SHIPMOOR).

The required physical model experiments have not been done to provide data to verify the accuracy of the multi-directional wave force and the damping simulations. More accurate roll drag coefficients may be available for use than the heavily approximated values used here, and they might be revealed by a thorough review of the experimental literature (which has not been attempted). There is therefore further developmental work remaining to be done before the developments can be regarded as being completed. In the meanwhile, the drag force representations implemented can be regarded as reasonable simple interim approximations to what is in reality a complicated system. Overall, the developments represent a significant increase in computational ship modelling capabilities that should enable more accurate simulations under a greater variety of environmental conditions in the future than has been possible hitherto.

7. REFERENCES

- 1 Spencer, JMA 'Time domain models of ships: Second-order mathematical model' HR Wallingford Report SR 418, March 1995
- 2 Bowers, EC and Spencer, JMA 'Set-down and surf beat in short crested seas: Comparison between theory and site measurement' HR Wallingford Report IT 272, August 1984
- 3 'Coefficients and procedures for predicting the effects of wind and current on VLCCs' Oil Companies International Marine Forum, 1975
- 4 Spencer, JMA 'Extrema of moored ship motions: Computational experiment study' HR Wallingford Report SR 502, May 1997

Tables

Table 1 Verification tests, results comparison: Significant motion values

Test Number	Inshore wave condition			Surge			Sway			Heave			Roll			Pitch			Yaw		
	Dir'n	H _s	T _m	Comp'l	Phys'l	Error %															
24	220	1.86	7.2	0.11	0.16	-31.4	0.14	0.12	19.3	0.07	0.11	-40.1	0.30	0.38	-21.6	0.15	0.13	18.3	0.15	0.13	11.6
23	220	2.39	8.2	0.18	0.27	-34.3	0.24	0.21	12.4	0.14	0.16	-12.8	0.50	0.65	-23.8	0.27	0.24	13.5	0.23	0.23	0.3
25	220	4.04	10.7	1.19	2.05	-41.9	0.79	1.09	-27.4	0.62	0.60	3.8	2.45	2.38	3.1	0.83	0.70	17.9	0.81	0.81	-0.1
7	243	2.07	7.2	0.09	0.17	-44.9	0.08	0.10	-21.3	0.04	0.08	-43.8	0.25	0.30	-18.3	0.10	0.10	4.9	0.10	0.09	7.5
8	243	3.07	8.8	0.43	0.48	-10.8	0.30	0.35	-14.3	0.21			0.80	0.91	-11.9	0.37	0.30	22.1	0.28	0.27	4.6
28	243	3.07	8.8	0.43	0.37	16.7	0.26	0.25	5.6	0.21	0.22	-3.0	0.79	0.86	-8.1	0.37	0.27	35.8	0.29	0.25	16.6
9	243	3.41	9.3	0.53	0.75	-28.8	0.36	0.44	-18.3	0.27			1.08	1.16	-7.3	0.42	0.37	13.8	0.33	0.34	-2.3
27	243	3.41	9.3	0.54	0.53	1.8	0.33	0.32	3.3	0.27	0.27	0.6	1.06	1.13	-6.0	0.42	0.33	27.7	0.34	0.33	3.1
26	243	4.05	10.2	1.47	1.17	25.4	0.60	0.57	5.9	0.49	0.43	15.1	1.89	1.71	10.4	0.67	0.49	36.1	0.55	0.53	4.4
11	243	4.61	10.9	2.87	2.64	8.6	0.90	1.33	-32.6	0.66	0.58	13.3	3.29	2.67	23.0	0.86	0.67	27.7	0.78	0.76	3.0
15	266	1.65	6.5	0.06	0.07	-13.7	0.03	0.08	-60.3	0.02	0.08	-75.8	0.14	0.20	-30.2	0.05	0.05	-9.6	0.05	0.07	-28.6
12	266	2.51	8.0	0.24	0.23	5.0	0.09	0.26	-66.9	0.08	0.20	-58.5	0.46	0.79	-42.2	0.16	0.22	-27.9	0.12	0.25	-52.2
13	266	2.81	8.5	0.31	0.31	-0.1	0.11	0.33	-66.1	0.13	0.24	-47.9	0.65	0.98	-33.2	0.21	0.27	-20.6	0.17	0.32	-48.3
14	266	3.40	9.4	1.00	0.60	67.2	0.25	0.58	-56.8	0.27	0.43	-38.2	1.43	1.72	-16.9	0.42	0.46	-9.7	0.30	0.55	-46.0
15'	266	1.65	6.5	0.06	0.07	-12.9	0.04	0.08	-44.7	0.02	0.08	-71.2	0.15	0.20	-23.2	0.06	0.05	10.9	0.07	0.07	-3.7
12'	266	2.51	8.0	0.25	0.23	10.1	0.11	0.26	-58.3	0.10	0.20	-50.7	0.63	0.79	-19.9	0.20	0.22	-6.9	0.17	0.25	-33.1
13'	266	2.81	8.5	0.43	0.31	37.7	0.14	0.33	-56.5	0.16	0.24	-35.3	0.83	0.98	-15.5	0.29	0.27	5.9	0.21	0.32	-33.5
14'	266	3.40	9.4	0.99	0.60	65.0	0.32	0.58	-44.1	0.34	0.43	-22.0	1.96	1.72	13.7	0.49	0.46	6.3	0.44	0.55	-20.1

Table 2 Verification tests, results comparison: Zero-crossing periods of motions

Test Number	Inshore wave condition			Surge			Sway			Heave			Roll			Pitch			Yaw		
	Dir'n	H _s	T _m	Comp'l	Exp'l	Error %															
24	220	1.86	7.2	16.2	13.6	18.9	14.8	11.3	31.0	9.3	17.2	-45.8	14.2	18.6	-23.6	8.7	8.8	-0.8	8.1	7.6	6.4
23	220	2.39	8.2	18.1	18.3	-0.9	17.5	13.3	31.3	10.2	10.2	0.3	15.5	23.0	-32.7	9.4	9.3	0.7	9.0	8.7	3.0
25	220	4.04	10.7	33.2	41.2	-19.4	19.6	22.5	-13.1	12.2	12.2	0.2	24.1	30.0	-19.7	11.1	11.0	1.1	12.3	11.9	3.3
7	243	2.07	7.2	17.2	10.5	63.9	11.6	9.3	24.3	9.3	28.3	-67.0	16.0	15.0	6.5	8.7	9.0	-3.9	8.0	6.0	32.8
8	243	3.07	8.8	26.5	26.8	-1.0	18.8	15.6	20.7	11.0	17.0	-35.6	19.6	24.4	-19.6	9.9	10.0	-1.1	9.7	10.0	-2.6
28	243	3.07	8.8	26.4	22.4	17.7	16.7	13.1	27.7	11.0	11.1	-1.4	19.4	24.3	-20.0	9.9	10.1	-2.1	9.7	10.0	-2.8
9	243	3.41	9.3	26.1	32.0	-18.4	18.6	18.0	3.3	11.3	17.4	-35.0	21.7	26.1	-16.7	10.1	10.3	-1.7	10.3	11.5	-10.6
27	243	3.41	9.3	25.8	27.0	-4.5	16.9	14.3	18.3	11.3	11.4	-0.8	21.2	26.0	-18.3	10.1	10.5	-3.6	10.2	11.2	-9.0
26	243	4.05	10.2	36.2	33.6	7.9	20.8	18.9	9.8	12.2	12.3	-1.1	21.6	27.9	-22.5	10.8	11.1	-3.1	11.8	12.6	-6.5
11	243	4.61	10.9	41.3	50.1	-17.7	23.0	26.0	-11.6	13.0	12.0	8.4	26.8	31.9	-16.0	11.4	11.3	0.9	13.1	14.5	-9.6
15	266	1.65	6.5	18.1	6.7	170.7	7.6	9.2	-17.1	8.8	15.7	-44.1	16.9	12.8	32.3	8.1	7.4	9.8	7.3	6.4	13.7
12	266	2.51	8.0	23.9	15.4	55.1	9.7	10.2	-5.4	10.4	11.3	-7.6	19.8	25.7	-23.0	9.4	9.2	2.1	8.8	9.0	-2.5
13	266	2.81	8.5	24.9	17.4	42.9	10.7	10.9	-1.7	10.8	11.1	-2.4	21.9	27.0	-18.9	9.8	9.3	5.2	9.3	9.7	-4.3
14	266	3.40	9.4	33.9	19.2	76.8	14.2	12.7	11.4	12.0	11.2	7.3	24.0	29.3	-18.2	10.3	10.1	1.7	10.4	11.2	-7.0
15'	266	1.65	6.5	16.93	6.7	152.7	7.6	9.2	-17.1	8.8	15.7	-44.2	13.7	12.8	7.0	8.2	7.4	10.1	7.2	6.4	12.7
12'	266	2.51	8.0	23.52	15.4	52.7	9.9	10.2	-3.2	10.4	11.3	-8.3	21.5	25.7	-16.3	9.3	9.2	1.4	8.8	9.0	-2.6
13'	266	2.81	8.5	27.31	17.4	57.0	10.8	10.9	-1.3	10.7	11.1	-3.3	22.6	27.0	-16.2	9.8	9.3	5.0	9.3	9.7	-3.6
14'	266	3.40	9.4	31.24	19.2	62.7	13.3	12.7	5.0	11.8	11.2	5.4	25.9	29.3	-11.5	10.4	10.1	3.2	10.5	11.2	-6.2

Figures

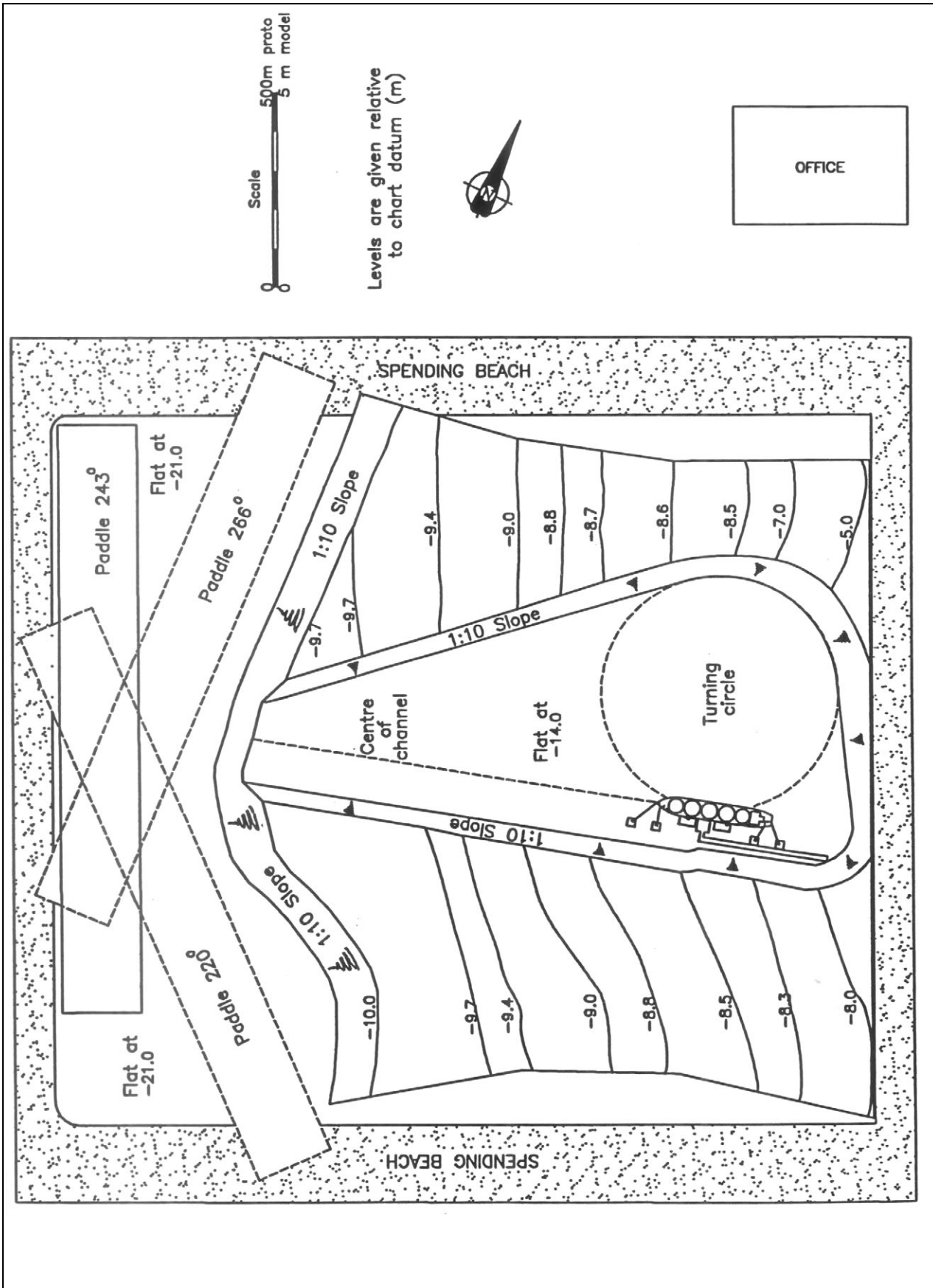


Figure 1 Physical model wave basin layout

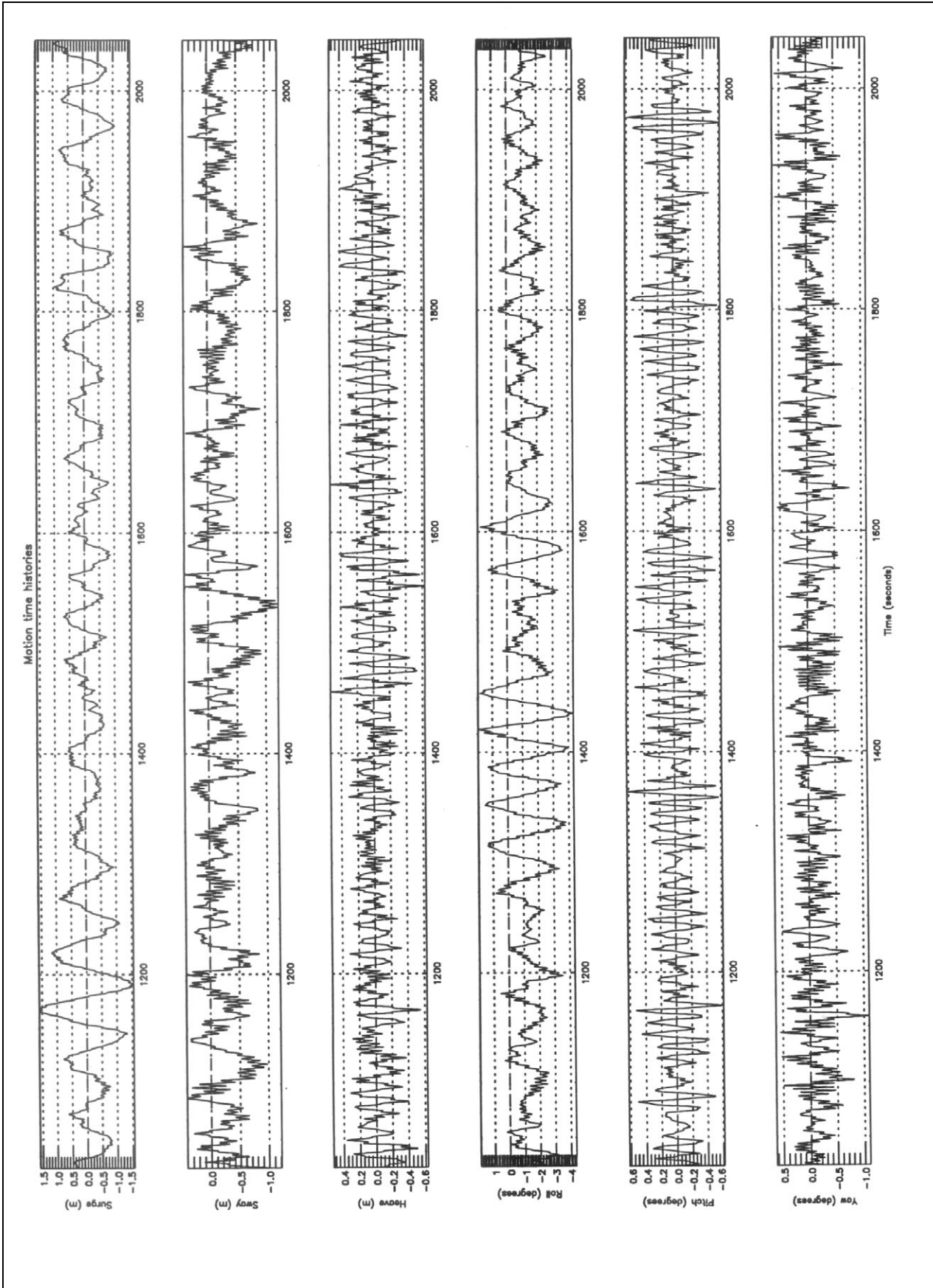


Figure 2 Motion time history plot

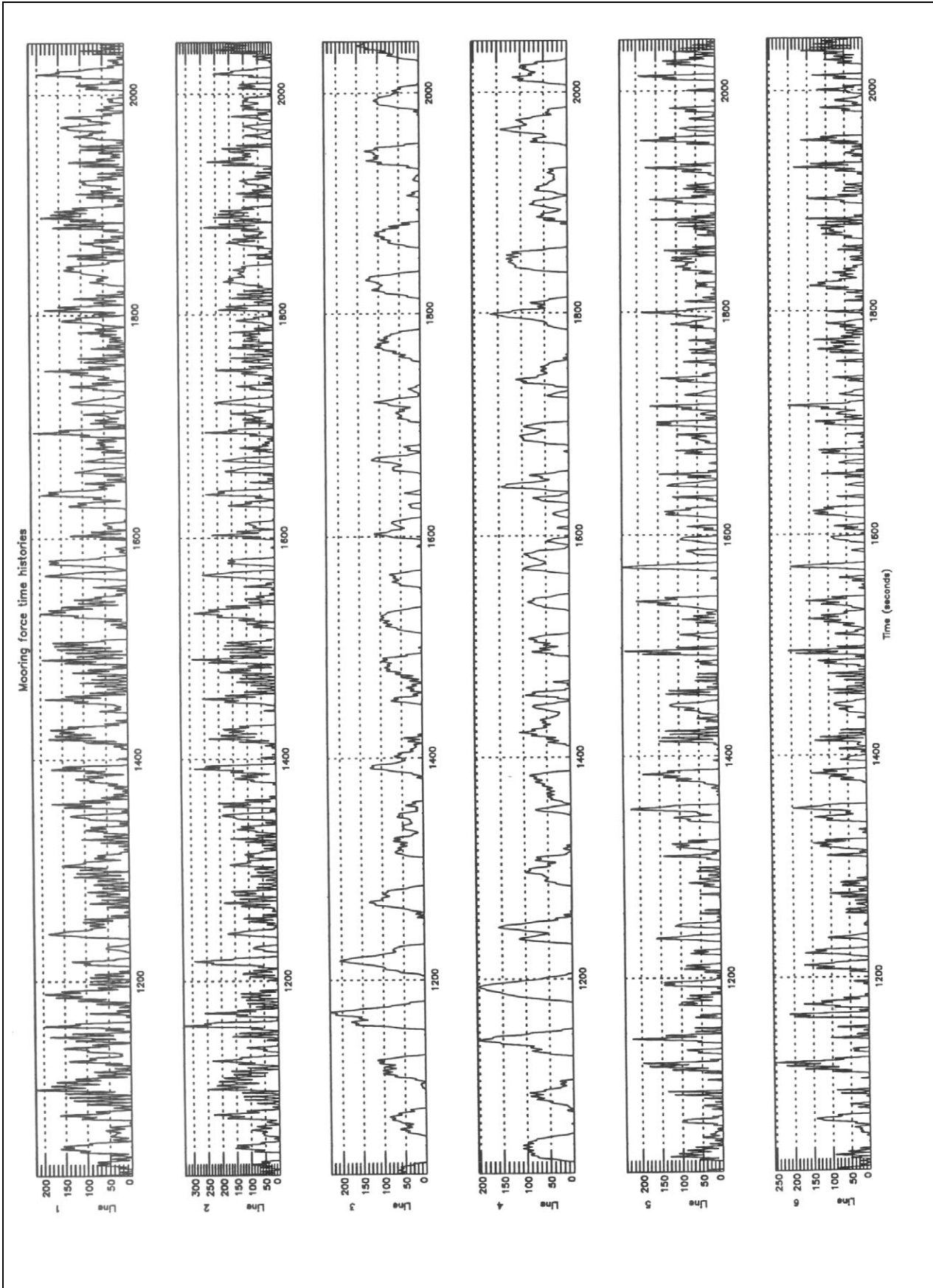


Figure 3 Mooring forces time history plot

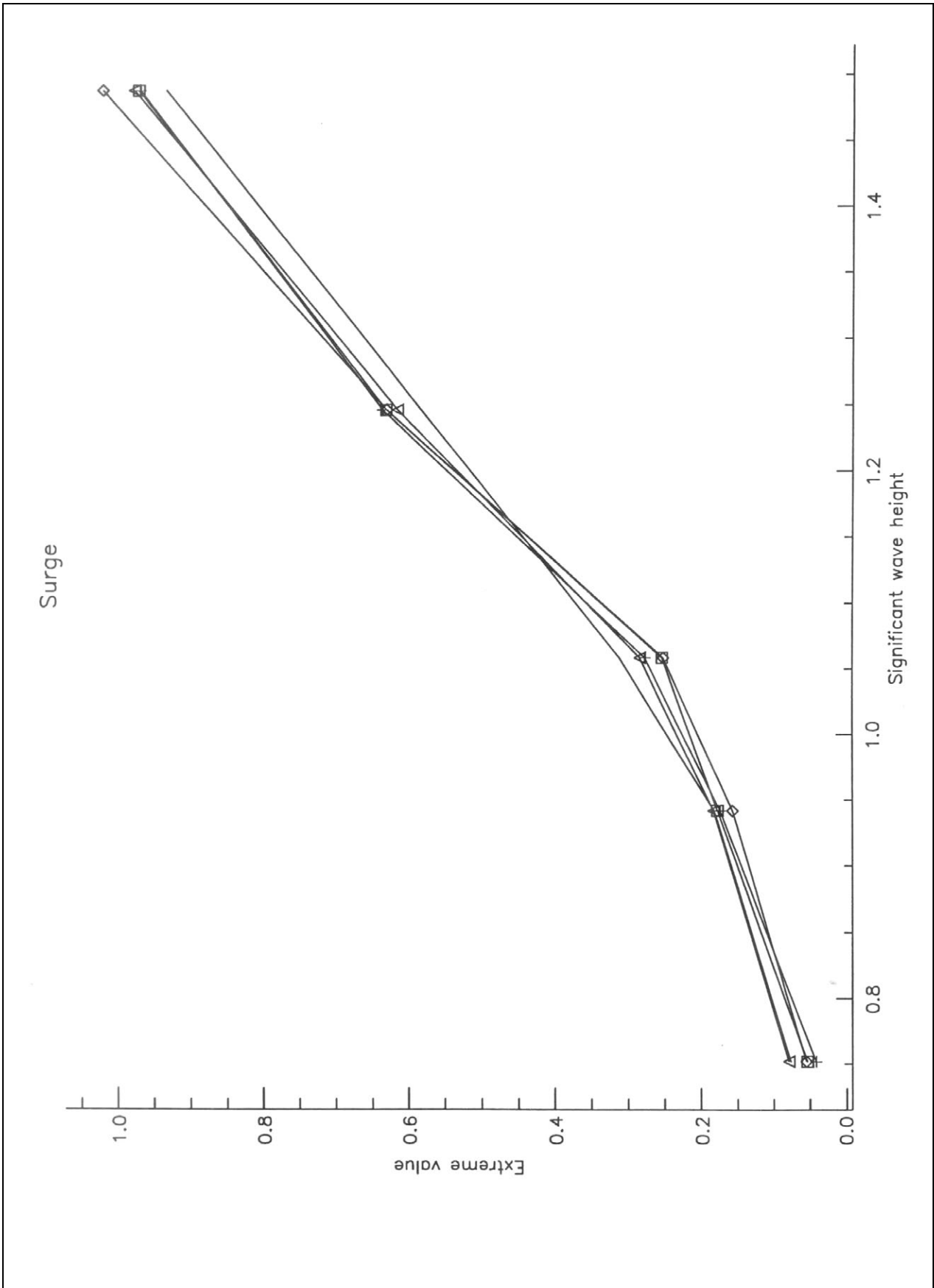


Figure 4 Results plot

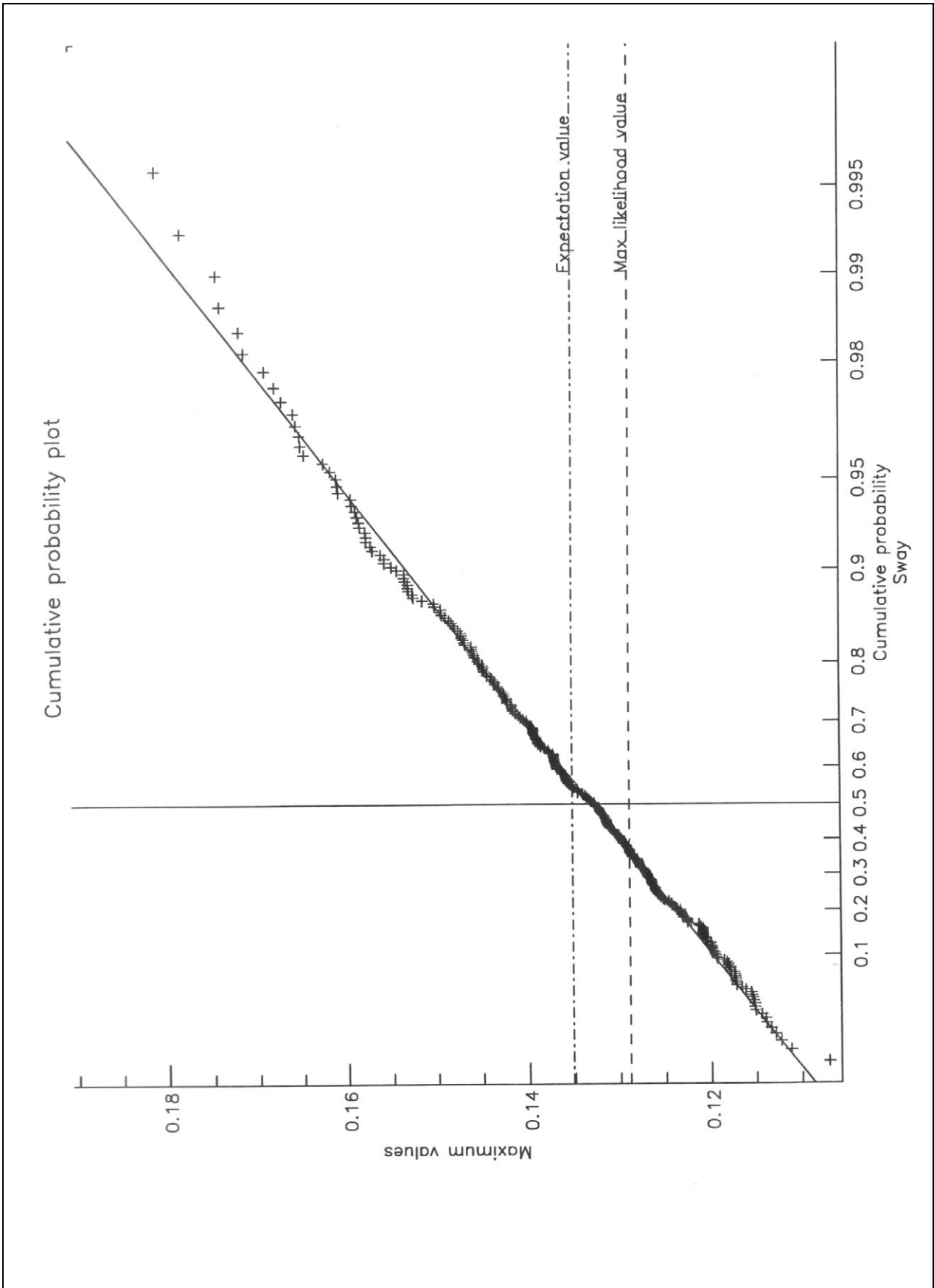


Figure 5 Extreme value plot

Appendices

Appendix 1

Interpolation of second-order force coefficients in a multi-directional sea

Appendix 1 Interpolation of second-order force coefficients in a multi-directional sea

A multi-directional wave signal can be represented as a Fourier transform:

$$\eta(\underline{x}, t) = \int_{\omega=-\infty}^{\infty} \int_{\theta=-\pi}^{\pi} a(\omega, \theta) e^{ik(x\cos\theta + y\sin\theta) - i\omega t} d\omega d\theta \quad 1$$

Where $a(\omega, \theta)$ is a complex Fourier coefficient corresponding to the wave component with radian frequency ω propagating in direction θ , and $a(-\omega, \theta) = a^*(\omega, \theta)$, with the superscript $*$ denoting complex conjugate.

Given a force coefficient function, $F(\omega_1, \omega_2, \theta_1, \theta_2)$, a second-order force signal in a multi-directional sea can be defined. (To obtain the difference frequency component, $\omega_1 - \omega_2$, frequency ω_2 is here in effect considered as being negative, hence its corresponding Fourier wave coefficient is complex conjugate.) :-

$$F^{(2)}(t) = \int_{\omega_1=-\infty}^{\infty} \int_{\omega_2=-\infty}^{\infty} \int_{\theta_1=-\pi}^{\pi} \int_{\theta_2=-\pi}^{\pi} F(\omega_1, \omega_2, \theta_1, \theta_2) a(\omega_1, \theta_1) a^*(\omega_2, \theta_2) e^{-i(\omega_1 - \omega_2)t} d\omega_1 d\omega_2 d\theta_1 d\theta_2 \quad 2$$

Note, $F(-\omega_1, -\omega_2, \theta_1, \theta_2) = F^*(\omega_1, \omega_2, \theta_1, \theta_2)$

Define a change of variables:

$$\text{Set: } \sigma = (\omega_1 + \omega_2)/2$$

$$\text{and } \delta = \omega_1 - \omega_2$$

$$\text{so } \omega_1(\sigma, \delta) = \sigma + \delta/2 \quad \omega_2(\sigma, \delta) = \sigma - \delta/2$$

Also define a force coefficient function $G(\sigma, \delta, \theta_1, \theta_2)$ so that:

$$G(\sigma, \delta, \theta_1, \theta_2) = F[\omega_1(\sigma, \delta), \omega_2(\sigma, \delta), \theta_1, \theta_2] \quad 3$$

With the change of variables, the integral expression for second-order force becomes:

$$F^{(2)}(t) = \int_{\sigma=-\infty}^{\infty} \int_{\delta=-\infty}^{\infty} \int_{\theta_1=-\pi}^{\pi} \int_{\theta_2=-\pi}^{\pi} G(\sigma, \delta, \theta_1, \theta_2) a(\sigma + \frac{1}{2}\delta, \theta_1) a^*(\sigma - \frac{1}{2}\delta, \theta_2) e^{-i\delta t} d\sigma d\delta d\theta_1 d\theta_2 \quad 4$$

This is similar to the form in which second-order forces and force coefficients are computed in DRIFTKEEL, with a primary wave frequency, σ , and difference frequency, δ .

The conjugate relationship applies: $G(-\sigma, -\delta, \theta_1, \theta_2) = G^*(\sigma, \delta, \theta_1, \theta_2)$

Now consider $G(\sigma, -\delta, \theta_1, \theta_2)$. This force coefficient arises from interactions of wave components with frequency $\sigma - \delta/2$ and direction θ_1 , and frequency $-\sigma - \delta/2$ and direction θ_2 ; write $[(\sigma - \delta/2, \theta_1), (-\sigma - \delta/2, \theta_2)]$.

However, the interactions of the two frequency-direction pairs are the same whichever order they are taken in; the interaction $[(\sigma - \delta/2, \theta_1), (-\sigma - \delta/2, \theta_2)]$ is the same in effect as $[(\sigma - \delta/2, \theta_2), (\sigma - \delta/2, \theta_1)]$, so:

$$G(\sigma, -\delta, \theta_1, \theta_2) = G(-\sigma, -\delta, \theta_2, \theta_1) \quad 5$$

So, since, from the conjugate relationship above, $G(-\sigma, -\delta, \theta_2, \theta_1) = G^*(\sigma, \delta, \theta_2, \theta_1)$:

$$G(\sigma, -\delta, \theta_1, \theta_2) = G^*(\sigma, \delta, \theta_2, \theta_1) \quad 6$$

This relationship is a generalisation of the one that applies to co-directional second-order force coefficients ($\theta_1 = \theta_2$) which was used in interpolation in the long-crested version of DRIFTKEEL:

$$G(\sigma, -\delta) = G^*(\sigma, \delta) \quad 7$$

The later interpolation stage in DRIFTKEEL referred to in the main text in Section 2.3 involves interpolating the function G for fixed values of σ , δ_1 and θ_2 across a range of values of the difference frequency, δ . The relationship above is used to extend the range of interpolation into the negative difference frequency (i.e. $\delta < 0$) region to improve accuracy and also computational efficiency - because the relationship has been established, interpolation needs only to be done for approximately half the possible number of (θ_1, θ_2) combinations.

Appendix 2

Sample Unix script for multiple test runs

Appendix 2 Sample Unix script for multiple test runs

The following is a sample of code to run multiple (in this case 50) test runs of SHIPMOOR and the associated DRIFTKEEL program for generating forcing time sequences in a Unix C-Shell environment.

```
1      touch maxvals
2      touch minvals
3      touch xtremvals
4      touch ranvals
5      touch rmsvals
6      touch rms0vals
7      foreach x ( q w e r t y u i o p )
8      foreach y ( 0 1 2 3 4 )
9      pushd TIMFOR_2c
10     nice +12 tf2 << +++++
11     75.
12     0.
13     .4
14     16k
15     90.
16     no
17     1. 4.
18     yes
19     no
20     no
21     +++++
22     popd
23     rm gr*p-tx
24     nice +12 TDM/tdm < moordat_aq_j90_ncurr_0kt+p-tx
25     fgrep -i 'largest value' op*p-tx | sed '1,45d' >> maxvals
26     fgrep -i 'smallest value' op*p-tx | sed '1,45d' >> minvals
27     fgrep -i 'extreme value' op*p-tx | sed '1,45d' >> xtremvals
28     fgrep -i 'range value' op*p-tx | sed '1,45d' >> ranvals
29     fgrep -i 'root mean' op*p-tx | sed '1,45d' >> rmsvals
30     fgrep -i 'rms from zero' op*p-tx | sed '1,45d' >> rms0vals
31     end
32     end
```

Commentary

Lines	Comments
1-6	Create files for storing results in. Creation beforehand is necessary in this case because data is written to these files by appending (see lines 25-30), and my (JMAS) standard C-Shell environment includes setting 'noclobber'.
7,8	Set two loops to perform following instructions a total of fifty times: ten times around the outer 'x' loop, five times around the inner 'y' loop.
9	Move to the 'TIMFOR_2c' directory where the force time sequence generation program resides.
10	Execute the force time sequence generation program

- 11-21 Data for the program
- 22 Move back to the original directory
- 23 Delete Ghost graphics files (no longer necessary using IDL)
- 24 Execute the SHIPMOOR program taking control and mooring data from file 'moordat_aq_j90_ncurr_0kt+p-tx'
- 25-30 Extract values required from the standard SHIPMOOR output and append them to the results files pre-created (lines 1-6). Extraction is done using fgrep to search for key character strings in the SHIPMOOR output file 'op*p-tx'. It is assumed there is only one file with a name matching the metacharacter - otherwise the name of the output file would need to be stated explicitly. The first forty-five occurrences of each string are then filtered out by piping through 'sed'; these are the results of partial analyses that pertain to only portions of the test run, and the required results are the final, overall values at the end of the output. The number of values needing to be filtered out depends on the length of a test run and the numbers of mooring lines and fenders; it is not always forty-five.
- 31,32 Terminations of loops that commenced at lines 7 and 8.